Photopolarimetric characterization of the transition between two turbulent states in a nematic liquid crystal film

G. Strangi,* C. Versace, N. Scaramuzza, D. E. Lucchetta, V. Carbone, and R. Bartolino
Dipartimento di Fisica, Università della Calabria and Istituto Nazionale per la Fisica della Materia (INFM), Unità di Cosenza, I-87036 Arcavacata di Rende (Cosenza), Italy
(Received 2 November 1998)

This work was aimed at the photopolarimetric characterization of the transition between two dynamic scattering modes that take place in a planarly aligned nematic liquid crystal sample, under the effect of an external low-frequency electric field. The time evolution of the degree of polarization and the behavior of the radiation entropy of the transmitted light allow us to interpret the transition between two turbulent states, or dynamic scattering modes, as a decay from a two-dimensional (2D) to a (3D) turbulence. [S1063-651X(99)10204-6]

PACS number(s): 61.30.−v, 83.70.Jr, 42.25.Ja

I. INTRODUCTION

During the past decade some progress has been achieved in understanding the formation and the dynamics of electrohydrodynamic patterns in nematic liquid crystals (NLC's) [1–3]. In particular, the transition between the two turbulent states called dynamic scattering modes (DSM's) has attracted the interest of a large number of scientists [4–8]. In this paper the ellipsometric characterization of this turbulence-turbulence transition, which takes place in a homogeneously aligned nematic sample under the action of an external electric field is reported. Up to now, to our knowledge, the measurements were effected detecting the intensity of the transmitted light during the formation of the dynamical patterns.

The ellipsometric technique allows a further characterization of the DSM1→DSM2 transition. This technique provides either information on the depolarization and on the decoherence effects of the polarization states of the transmitted light, because of the random variations of the field director. The effects of decoherence and of depolarization of the transmitted light were monitored recording the time behavior of the Stokes parameters of the radiation and the time evolution of the degree of polarization P [9].

II. EXPERIMENT

The experiment consists of the application of an alternate electric field (freq=70 Hz) across a planarly aligned NLC film. The main purpose is the observation of electrohydrodynamic instabilities. The sample cell, as shown in Fig. 1, consists of two semitransparent (sputtered ITO) electrodes, which are spaced by a Mylar mask 36 μm thick. Both surfaces of the cell are coated by polymeric film (ACM-72) that is mechanically rubbed to induce a mean molecular orientation parallel to the surfaces (the x direction). The cell is filled by the nematogen compound MBBA.

Electrohydrodynamic convection (EHC) originates in a NLC layer subject to an alternating external voltage V_0. The first instability of the basic unstructured director field occurs, as a result of two forces: a pure dielectric restoring torque due to the negative dielectric anisotropy and a force exerted on the bulk fluid due to the charges separation produced by the positive conductive anisotropy [10]. Just above a certain threshold voltage V_1 (for our sample $V_1=6.8$ V) the instability produced by the occurrence of both forces leads to a periodic pattern of convective roll structures connected with periodic distortion of the director. The hydrodynamic motion is not visible directly but becomes manifest because of the anisotropy in the index of refraction. When V_0 is further increased transitions to more complicated spatiotemporal states are observed [11–13]. The various bifurcations lead to the different patterns that are strongly influenced by the presence of defects. When a second threshold voltage V_2 is reached (for our sample $V_2=28$ V) a transient bimodality from a first turbulent regime (DSM1) to a second turbulent regime (DSM2) occurs [14].

We characterized the DSM states by studying the polarization of the transmitted light by a Division of Amplitude Photopolarimeter (DOAP). The DOAP allows the simultaneous measurement of the Stokes parameters, usually denoted by S_0, S_1, S_2, S_3, representing the different possible states of polarization of a quasimonochromatic wave [15]. The direct measurements of the Stokes parameters permit us to determine the degree of polarization P,

$$P=\left[\sum_{k=1}^{3}\left(\frac{S_k}{S_0}\right)^2\right]^{1/2}. \tag{1}$$

P varies from zero for unpolarized light to unity in the case of totally polarized light and assumes intermediate values for

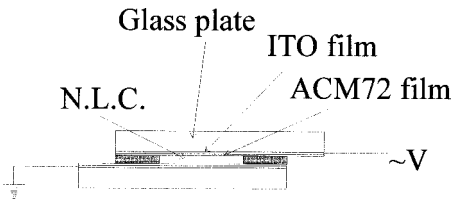

FIG. 1. The nematic liquid crystal cell.

*Author to whom correspondence should be addressed. Electronic address: Strangi@fis.unical.it

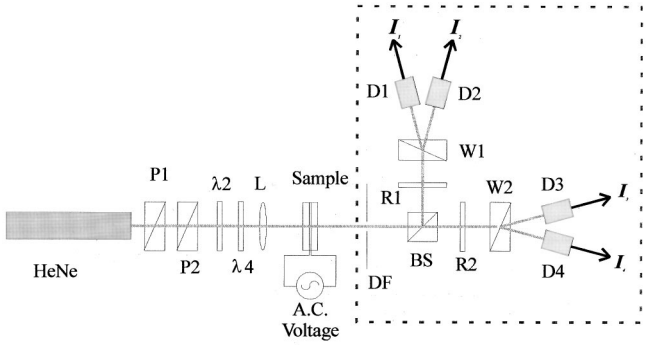

FIG. 2. The experimental setup: $P1$ and $P2$ linear polarizers, λ2 half-wave retarder, λ4 quarter-wave retarder, L convergent lens ($f = 300$ mm), $R1$ and $R2$ quarter-wave retarders, $W1$ and $W2$ Wollaston prisms, $D1, D2, D3$, and $D4$ linear detectors, beam splitter (BS) and diaphragm (DF). The dotted rectangle surrounds the DOA Photopolarimeter.

partially polarized light. The degree of polarization P may be viewed as an order parameter indicating the degree to which the wavefield is ordered.

In Fig. 2 is shown the DOAP that has been implemented in our laboratory. This device was originally conceived by Azzam [16]; it is capable of measuring simultaneously the four Stokes parameters and thus can work with totally polarized light as well as with partially polarized light. The key element is a polarizing beam splitter that divides an incident beam under measurement i into a reflected beam r, and a transmitted beam t; the intensities in two orthogonal transverse direction of the reflected and transmitted beams are measured by Wollaston prisms $W1$ and $W2$, which are followed by the linear photodetectors $D1$,$D2$,$D3$,$D4$. The instrument has a fast response (limited only by the speed of the photodetectors), it has not any moving parts and does not require modulation.

The light source is a 2-mW He-Ne laser ($\lambda = 632.8$ nm), the light intensity can be adjusted by means of a variable attenuator that consists of two linear polarizers $P1$ and $P2$. The calibration of the instrument requires at least three linearly polarized states and one circularly polarized state; therefore we use a half-wave retarder λ2 followed by a quarter-wave retarder λ4, which allows us to obtain any polarization state. A thermostatic bath guaranteed a temperature stability of better than 0.1 °C.

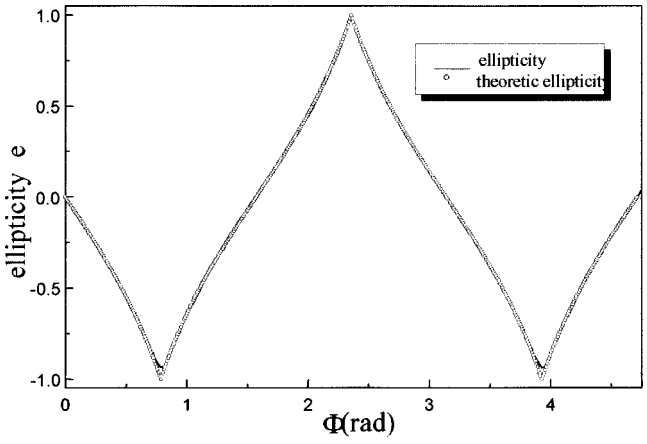

FIG. 3. A test run, the ellipticity e of a light beam transmitted by the quarter-wave retarder λ4 as a function of the rotation angle ϕ of its optical axes. In other words, ϕ is the angle between the optical axes of λ2 and the optical axes of λ4.

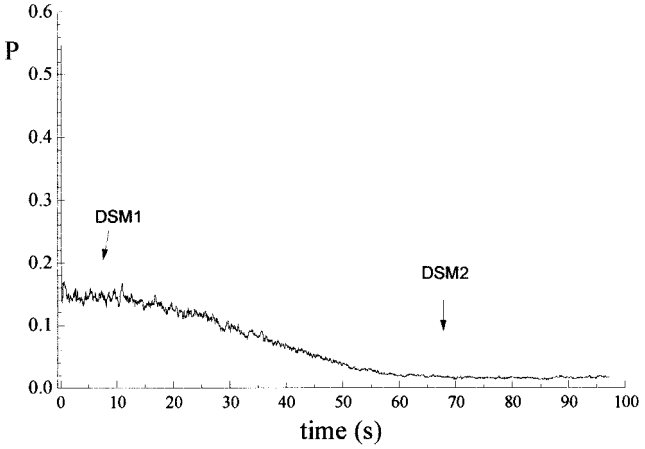

FIG. 4. The degree of polarization P of the light transmitted versus time. The applied voltage was $V_0 = 32.0$ V root mean square, the incident light was linearly polarized perpendicularly to the planar anchoring direction and the oven temperature 24.0 °C.

The light beam is focused on the sample by the lens L ($f = 300$ mm); the resulting spot size is approximately 250 μm. The large area (100 mm^2) photodiodes $D1$, $D2$, $D3$, and $D4$, which operate in photovoltaic mode, generate the electric signals $I1$,$I2$,$I3$,$I4$ that are acquired by a 16-bit multifunction board (Microstar Laboratories DAP 1216e); a personal computer provides the data storage and elaboration.

Following Azzam [16] the calibration of the DOAP was effected for 11 different positions of λ2 and λ4 that correspond to three linearly polarized states and eight circularly polarized states. After the calibration, the photopolarimeter was tested rotating a quarter-wave retarder placed between the source, opportunely polarized, and the DOAP obtaining the curve shown in Fig. 3, where the ellipticity is reported vs the quarter-wave retarder rotation angle Φ. As comparison the experimental ellipticity is plotted together to the theoretic ellipticity e_{TH}:

$$e_{\mathrm{TH}} = \tan\left\{ \tfrac{1}{2} \arcsin\left[\frac{\sin 2\Phi}{(\tfrac{1}{2} + \tfrac{1}{2}\cos 4\Phi + \sin^2 2\Phi)^{1/2}} \right] \right\}. \quad (2)$$

Equation (2) was calculated by means of the normalized Stokes parameters, given as function of Φ [17].

III. TRANSITION BETWEEN THE TURBULENT STATES DSM1-DSM2

The application of a low-frequency electric field across the cell give rise to the formation of well-known electrohydrodynamic patterns. Our interest was turned to the DSM regimes. Observations have already shown in early time that there are two different kinds of DSM in planar orientation of the NLC, the DSM1, and the DSM2 states.

We characterize both states by measuring the time evolu-

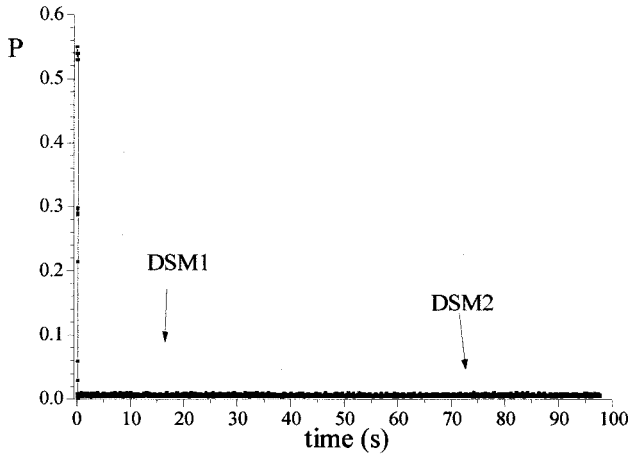

FIG. 5. The same as Fig. 4 but with the incident light polarized along the planar anchoring direction.

tion of the degree of polarization P of the transmitted light during the transition DSM1→DSM2. The mean reason for this measurement is related to the depolarization effects of the turbulent regimes.

In fact, the decorrelation of the phases and amplitudes of the wave-field components is responsible for the depolarization of the probe beam. When the parameters of the external perturbation were increased slightly above the threshold for the DSM1-DSM2 transition, an incident linear polarization state along the Y direction was selected, i.e., orthogonal to the direction of anchorage of the molecules. The time evolution of degree of polarization P is shown in Fig. 4. As can be seen in the DSM1 regime the transmitted light by the sample is only partially depolarized ($P \cong 0.2$) with respect to the condition of absence of electric field ($P_{(V=0)} \cong 0.55$). Holding constant V_0 and maintaining unaffected all the other experimental conditions, after a certain time interval that depends on V_0 (approximately 10 sec at $V_0 - V_2 = 4$ V) the DSM2 occurs. During the transient P monotonically decrease and when the DSM2 spreads all over the cell the light is nearly totally depolarized ($P < 0.03$).

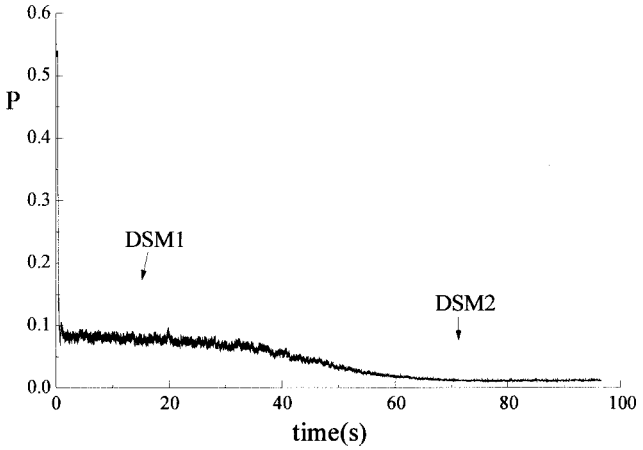

FIG. 6. The same as Fig. 5 but with the incident light circularly polarized.

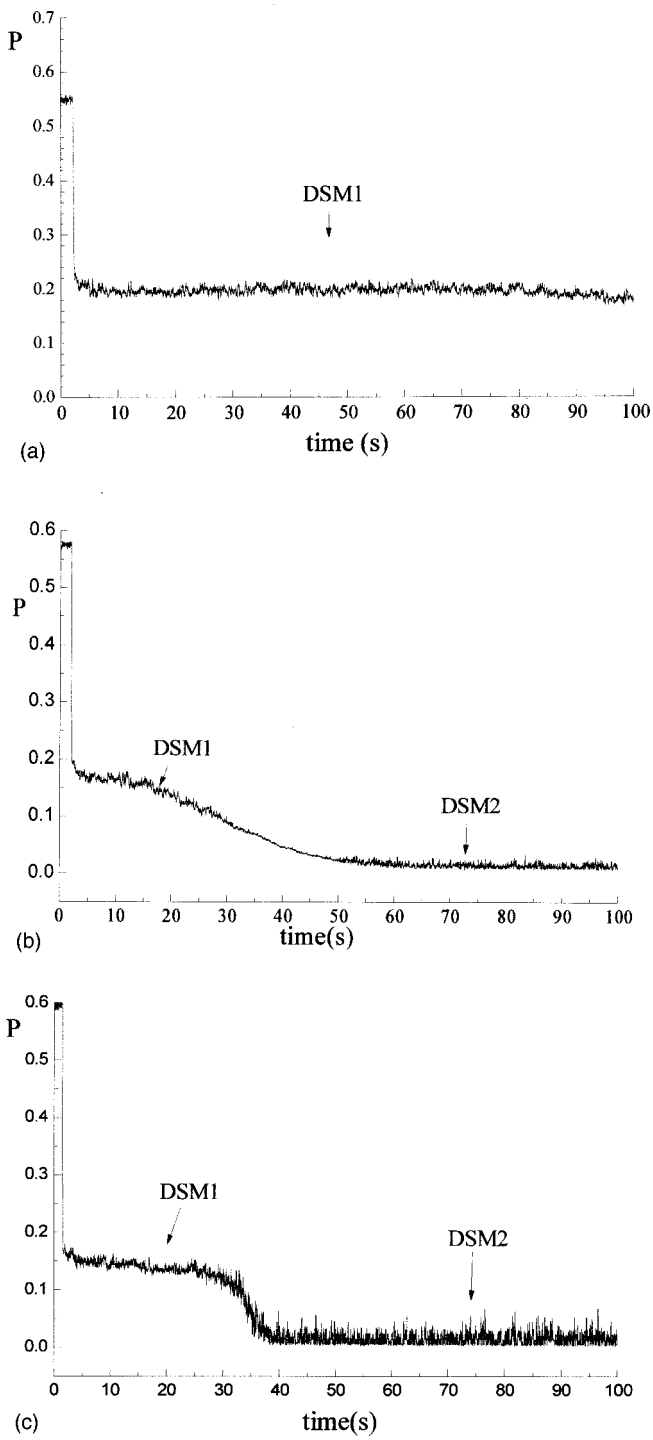

FIG. 7. A comparison among different applied voltage. Below the DSM1→DSM2 threshold, $V_0 = 28$ V [Fig. 7(a)]; $V_0 = 35$ V [Fig. 7(b)]; $V_0 = 40$ V [Fig. 7(c)].

The behavior we have described is essentially due to the fact that the small hydrodynamic loops that are responsible for the DSM1 regime cause a massive motion of the molecular director that remains predominantly in the x-z plane, i.e., the plane that contain the unperturbed direction of the director. For this reason the fluctuations of the refraction indexes have still a certain degree of correlation, while in the DSM2 regime the hydrodynamic loops become randomly oriented in the sample and the variations of the refraction indexes show a lowest degree of correlation; the direct consequence

of this fact is the total depolarization of the light. On the other hand, if the incident polarization state lies along the x direction, i.e., parallel to the plane containing the original undistorted orientation of the molecular director, P is practically zero both in the DSM1 and in the DSM2, as we can see in Fig. 5. This confirms that, also in the DSM1, along the x direction there is a total absence of coherence in the fluctuations of the field director.

These considerations find a subsequent confirmation in the measurement shown in Fig. 6, that has been effected with circularly polarized light. Considering that circularly polarized light average the informations over all directions, the value of P during the DSM1 is intermediate to those measured with light linearly polarized along the x and y directions. As shown in Figs. 7(a)–7(c), where P is reported for different value of V_0 and light polarized along y, the degree of polarization strongly depends on the applied voltage, in particular P decreases when V_0 increases in both the DSM1 and DSM2 regimes.

A point of further interest is to characterize the polarization of optical waves propagating through a scattering medium [18,19] and the entropy production during the DSM1-DSM2 transition. In trying to understand depolarization, it is useful to consider two main approaches [20]. The selective absorption of polarization states is the first approach. The second approach preserves total flux and induces depolarization by decorrelation of the phases and amplitudes of the electric field components; it is essentially an entropic effect arising from the irreversible evolution of the polarization state during the DSM.

The radiation entropy defined following von Neumann is analytically related to the degree of polarization of the field; note that the radiation entropy with which we will be concerned here is of a different nature than the spectral entropy derived from Planck's formula [21]. The radiation entropy S in the von Neumann measure is associated to the coherence matrix W [22]:

$$S(W) = -\mathrm{tr}[W(\ln W)]; \tag{3}$$

it takes a simple analytical expression when $\mathrm{tr}(W) = 1$, which is the case to be considered here:

$$S(P) = -\ln[c(P)], \tag{4}$$

with

$$c(P) = \tfrac{1}{2}(1+P)^{(1+P)/2}(1-P)^{(1-P)/2}. \tag{5}$$

It is worth mentioning that (i) the entropy in Eq. (4) depends only on P and not on the detailed state of polarization; (ii) it satisfies the inequalities

$$S(P=1) \leqslant S \leqslant S(P=0). \tag{6}$$

The quantity S calculated for the same data of Figs. 7(a) and 7(b) is shown in Figs. 8(a) and 8(b). We can observe in Fig. 8(a) that when the voltage is switched on, below V_2, the radiation entropy sharply increases and subsequently remains constant. In Fig. 8(b) we show that S further increase during the DSM1→DSM2 and reaches a saturation level $S(P \cong 0)$.

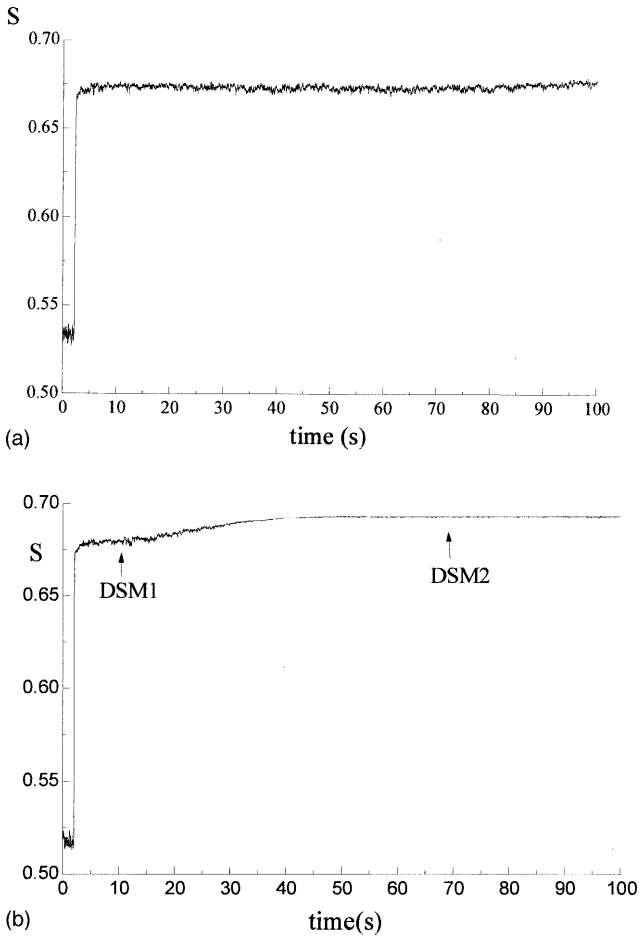

FIG. 8. The radiation entropy S versus the time. Below the DSM1→DSM2 threshold $V_0 = 28$ V [Fig. 8(a)]. Above the threshold $V_0 = 35$ V [Fig. 8(b)].

IV. CONCLUSIONS

In this work is reported the photopolarimetric characterization of the dynamic scattering modes that take place in a planarly aligned nematic liquid crystal sample (MBBA) under the effect of an external alternate electric field. The study was effected by measuring the Stokes parameters of the light transmitted by the turbulent sample.

These measurements have been performed by a Division of Amplitude Photopolarimeter that provide the Stokes parameters of the radiation. The degree of polarization P is a suitable parameter for the characterization of the different turbulent dynamical regimes. Our principal conclusion is that P drastically depends on the orientation of the polarization plane of the light impinging on the sample.

During the DSM1, if the direction of polarization is normal to the direction of the planar anchoring, the light is only partially depolarized ($P \cong 0.2$) with respect to the condition of absence of electric field ($P_{(V=0)} \cong 0.55$). In the DSM2 the light is totally depolarized; in fact, during the DSM1→DSM2 transition P decreases rapidly. On the other hand, if the direction of polarization lies along the direction

of the planar anchoring, the light is totally depolarized also in the DSM1 state and the time behavior of P does not reveal any trace of the turbulence-turbulence transition.

That is, in the dynamic regime DSM1 the turbulent structures remain predominantly in the x-z plane and it may be viewed like the overlap of many elementary vortexes, in which the fluctuations of the field-director happens essentially in the plane that contains the direction of anchorage. Only after the transition to the second dynamic scattering regime, the orientation of these elementary vortexes could be isotropic in the space, so that only in the DSM2 the turbulence is fully structureless. Therefore we could consider the DSM1→DSM2 like a transition from a structured 2D turbulence towards a structureless 3D turbulence.

[1] M. C. Cross and P. C. Henberg, Rev. Mod. Phys. **65**, 851 (1993).

[2] P. G. de Gennes and J. Proust, *The Physics of Liquid Crystals* (Oxford University Press, New York, 1993).

[3] L. M. Blinov and V. G. Chigrinov, *Electrooptic Effects in Liquid Crystal Materials* (Springer-Verlag, New York, 1994).

[4] S. Kai, W. Zimmerman, A. Masanori, and N. Chirumi, Phys. Rev. Lett. **64**, 1111 (1990); S. Kai and W. Zimmerman, Prog. Theor. Phys. Suppl. **99**, 458 (1989).

[5] S. Kai, K. Hayashi, and Y. Hidaka, J. Phys. Chem. **100**, 19 007 (1996).

[6] S. Kai, M. Andoh, and S. Yamaguchi, Phys. Rev. A **46**, R7375 (1992).

[7] S. Kai and W. Zimmermann, Phys. Rev. A **46**, 4954 (1992).

[8] N. Scaramuzza, C. Versace, and V. Carbone, Mol. Cryst. Liq. Cryst. **266**, 85 (1995).

[9] R. M. A. Azzam and N. M. Bashara, *Ellipsometry and Polarized Light* (North-Holland, Amsterdam, 1987).

[10] W. Helfrich, J. Chem. Phys. **51**, 4092 (1969).

[11] A. Joets and R. Ribotta, Physica D **23**, 235 (1986).

[12] S. Rasenat, V. Steinberg, and I. Rehberg, Phys. Rev. A **42**, 5998 (1990).

[13] A. Joets and R. Ribotta, Phys. Rev. Lett. **60**, 2164 (1988).

[14] V. Carbone, N. Scaramuzza, and C. Versace, Physica D **16**, 314 (1997).

[15] R. M. A. Azzam, Opt. Acta **32**, 1407 (1985).

[16] R. M. A. Azzam, Opt. Acta **29**, 685 (1982).

[17] R. M. A. Azzam, E. Masetti, I. M. Elminyawi, and F. G. Grosz, Rev. Sci. Instrum. **59**, 84 (1988).

[18] I. Freund, Opt. Commun. **81**, 251 (1991).

[19] I. Freund, M. Kaveh, R. Berkovitz, and M. Rosenbluh, Phys. Rev. B **42**, 2613 (1990).

[20] C. Brosseau, Optik (Stuttgart) **88**, 109 (1991).

[21] R. C. Jones, J. Opt. Soc. Am. **43**, 138 (1953); see also N. D. Gudkov, Opt. Spektrosk. **68**, 224 (1990) [Opt. Spectrosc. **68**, 130 (1990)].

[22] M. Born and E. Wolf, *Principles of Optics* (Pergamon, Oxford, 1980).